Acknowledgment

The author wishes to acknowledge the assistance given him by Prof. A. Papoulis, Polytechnic Institute of Brooklyn, who guided the initial study. The author also wishes to acknowledge the helpful contributions of L. Susman and J. Hanley of the Sperry Gyroscope Co., New York, during the study phase supported by the USAF.

References

[1] W. Getsinger, "Analysis of certain transmission-line networks in the time domain," *IRE Trans. on Microwave Theory and Techniques*, vol. MTT-8, pp. 301–309, May 1960.
[2] J. Reed and G. Wheeler, "A method of analysis of symmetrical four-port networks," *IRE Trans. on Microwave Theory and Techniques*, vol. MTT-4, pp. 246–252, October 1956.
[3] S. Dunn, and G. Ross, "Signal flow and scattering techniques in microwave network analysis," *Sperry Engrg. Rev.*, vol. 12, pp. 10–22, December 1959.
[4] A. Friebig, "Lineare signal fluidiagramme," *Arch. Elek. Ubertr.*, vol. 15, pp. 285–292, June 1961.
[5] S. Mason, "Feedback theory—further properties of signal flow graphs," *Proc. IRE*, vol. 44, p. 920–926, July 1956.
[6] F. Kuo, *Network Analysis and Synthesis*. New York: Wiley, 1962, p. 193.
[7] J. Truxal, *Control System Synthesis*. New York: McGraw-Hill, 1955, p. 509.
[8] G. Ross and L. Schwartzman, "Continuous beam steering and null tracking with a fixed multiple-beam antenna array system," *IEEE Trans. on Antennas and Propagation*, vol. AP-12, pp. 541–551, September 1964.
[9] H. Hall and S. Knight, *Higher Algebra*. New York: Macmillan, 1960, p. 484.
[10] J. Butler and R. Love, "Beam forming matrix simplifies the design of electronically scanned antennas," *Electronic Design*, vol. 9, pp. 170–173, April 1961.
[11] C. Montgomery, R. Dicke, and E. Purcell, *Principles of Microwave Circuits*, M.I.T. Rad. Lab. Ser., vol. 8, New York: McGraw-Hill, 1947, p. 308.
[12] K. Mortenson, "Microwave semiconductor control devices," *Microwave J.*, vol. 7, pp. 53–61, July 1964.
[13] "Time domain reflectometry," Hewlett-Packard Company, Palo Alto, Calif., Application Note 62, 1964.
[14] G. Ross, "The synthetic generation of phase-coherent microwave signals for transient behavior measurements," *IEEE Trans. on Microwave Theory and Techniques*, vol. MTT-13, pp. 704–706, September 1965.
[15] G. Ross, L. Susman, and J. Hanley, "Transient behavior of large arrays," Rome Air Development Center, New York, Tech. Rept. RADC-TR-64-581, USAF Contract AF30(602)-3348, June 1965.
[16] G. Ross, "The transient analysis of multiple beam feed networks for array systems," Ph.D. dissertation, Polytechnic Institute of Brooklyn, Brooklyn, N. Y., 1963.

Slit-Coupled Strip Transmission Lines

S. YAMAMOTO, STUDENT MEMBER, IEEE, T. AZAKAMI, MEMBER, IEEE, AND K. ITAKURA

Abstract—Two types of slit-coupled strip-line configuration are presented which are especially useful for the realization of multisection components using printed-circuit techniques. The slit-coupled configurations described consist of a pair of strips oriented face to face and either parallel or perpendicular to the outer ground planes. Coupling is achieved through a longitudinal slit. Exact conformal mapping solutions of the even- and odd-mode characteristic impedances are arranged in the forms of the design equations for both parallel and perpendicular cases. In order to facilitate design, nomograms are presented for the parallel case which give the physical line dimensions in terms of the even- and odd-mode characteristic impedances. Furthermore, the exact design equations for both parallel and perpendicular broadside-coupled strip configurations, which are considered to be special cases of the slit-coupled configurations, are presented. Formulas for the terminating lines are also included. The proposed parallel-coupled strip transmission line configurations permit smooth variation of coupling and applications to a wide variety of circuit components.

Manuscript received May 2, 1966; revised August 4, 1966.

S. Yamamoto and K. Itakura are with the Department of Electrical Communication Engineering, School of Engineering, Osaka University, Osaka, Japan.

T. Azakami is with the Nara Technical College, Nara, Japan. He was formerly with the Dept. of Electrical Communication Engineering, School of Engineering, Osaka University.

Introduction

A NUMBER of approaches to the distributed coupling effect between parallel conductors have been proposed, and applications have been made to the various circuit components, such as filters [1]–[4], directional couplers [5]–[9], channel separation filters [10]–[12], phase shifters [13], delay equalizers [14], [15], and hybrid circuits [16]–[18]. Most of these components make use of multisection-coupled transmission lines in order to provide the desired circuit performances over a wide frequency range. Typical configurations of the coupled transmission line multisection components are illustrated in Fig. 1. Combinations of these connecting types are also employed. Usually the canonical coupled sections to be connected have different coupling characteristics and close coupling is required in many practical cases.

Simple coupled strip-line configurations of the close coupling type, applicable to printed-circuit constructions, are the broadside-coupled configurations [19] shown in Fig. 2(a) for the parallel case, and in Fig. 2(b) for the perpendicular case. While design equations are available [19], [20], they are not suited to the realiza-

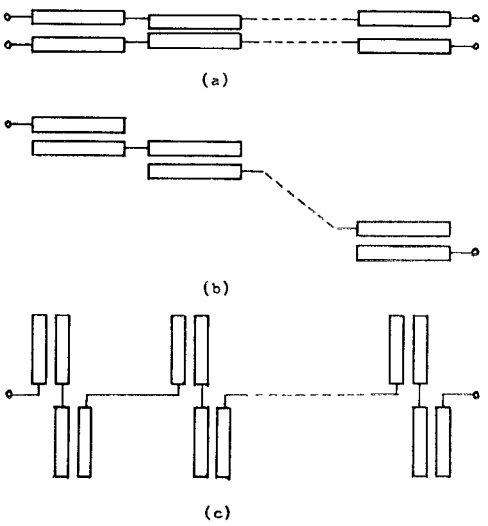

Fig. 1. Typical configurations of coupled transmission line multisection components.

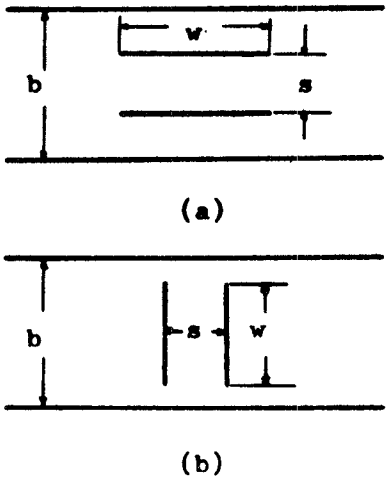

Fig. 2. Broadside-coupled strip transmission lines. (a) Parallel case. (b) Perpendicular case.

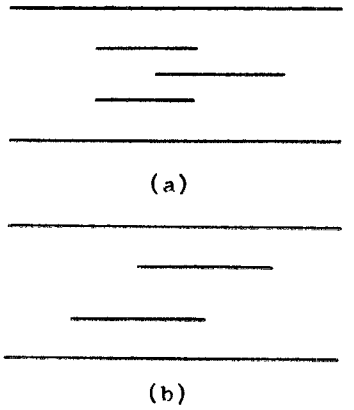

Fig. 3. Cross sections of coupled strip transmission lines suitable for the multisection components in Fig. 1(a).

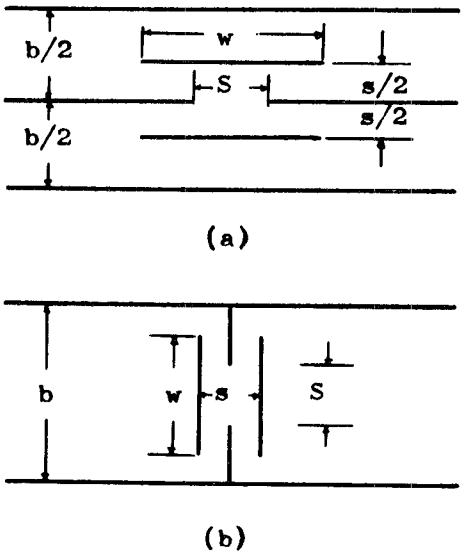

Fig. 4. Cross-section dimensions of slit-coupled strip transmission lines. (a) Parallel case. (b) Perpendicular case.

tion of the multisection components since the strip spacing varies as the coupling varies in these configurations. Close coupling configurations for printed-circuit constructions, well suited to the multisection components, as in Fig. 1(a), have been proposed by Getsinger [21] and Shelton [22]. The cross-sectional views of these configurations are shown in Fig. 3(a) and (b). For both configurations, design data based on the approximate conformal mapping solutions have been given. These configurations, however, are not always the desirable ones since it is difficult to construct the multisection components, such as those in Figs. 1(b) and (c), by using them. Furthermore, there exist certain limitations on physical line dimensions because of the approximations used in the derivations of the fringing capacitances.

The purpose of the present paper is to present the design data for slit-coupled configurations consisting of zero thickness conductors, as shown in Fig. 4(a) for the parallel case, and in Fig. 4(b) for the perpendicular case. In both cases, there are two parallel strips, two parallel outer ground planes of infinite width, and an inner ground plane having a longitudinal slit. These configurations may be considered to be modifications of the broadside-coupled ones of Fig. 2(a) and (b). They are used, however, to allow the coupling variation to be achieved by varying the slit width with constant strip spacing, and are applicable to the realization of the multisection components as in Fig. 1(a), (b), and (c). Furthermore, exact design equations can be obtained for both of these configurations and, therefore, no limitation on characteristic impedances or physical dimensions exists. This paper also presents the exact design equations for broadside-coupled configurations, which are derived by simple modification of the equations for slit-coupled ones. By the use of the equations for broadside-coupled cases, maximum values of coupling of slit-coupled cases can be found for given values of strip spacing.

Design equations considering the thickness of the conductors are not given here, but it is possible to derive them approximately by the familiar methods, such as those used by Arakawa [23] and Cohn [24].

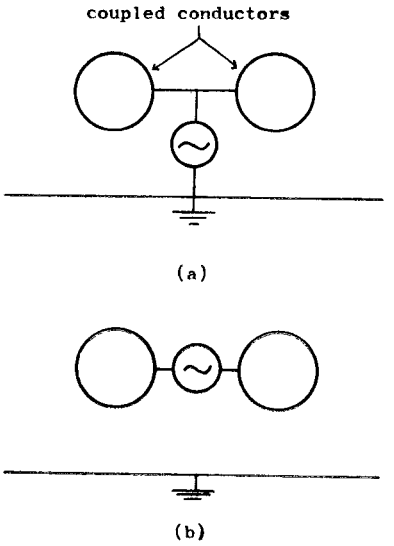

Fig. 5. Excitations of the fundamental modes in a parallel-coupled transmission line. (a) Even-mode. (b) Odd-mode.

Fundamental Modes and Characteristic Impedances of a Parallel-Coupled Transmission Line

We consider a lossless symmetrical parallel-coupled transmission line with the cross section uniform and the medium surrounding the conductors assumed homogeneous and isotropic with permittivity ϵ and relative permittivity ϵ_r. Then two orthogonal TEM modes can propagate along such a structure. These fundamental modes are usually denoted as the even-mode, in which equal currents flow on the two conductors in the same direction, and the odd-mode, in which equal currents flow in the opposite directions, as shown in Fig. 5. As a consequence of the line geometry, the plane of symmetry may be replaced by a magnetic wall in the even-mode and by an electric wall in the odd-mode. The even- and odd-mode characteristic impedances, Z_{oe} and Z_{oo}, for one conductor can be related to the static capacitances per unit length by

$$\sqrt{\epsilon_r} Z_{oe} = \frac{120\pi}{(C_{oe}/\epsilon)}$$

$$\sqrt{\epsilon_r} Z_{oo} = \frac{120\pi}{(C_{oo}/\epsilon)}, \tag{1}$$

where C_{oe} = static capacitance of one conductor to ground per unit length in the even-mode, and C_{oo} = that in the odd-mode. The performance of the coupled transmission line may be completely described in terms of these characteristic impedances. Note that for the coupled two-conductor line with common return under consideration,

$$Z_{oe} \geqq Z_{oo}. \tag{2}$$

Design Equations

Among various methods that exist for the evaluation of the static capacitances and, therefore, the characteristic impedances, of the TEM-mode transmission lines, the conformal mapping and the variational methods are typical. However, by the use of the variational method, the solutions, in general, are not obtained in closed forms and, therefore, it is difficult to get the design equations that are of importance in the design of the circuit components. Hence, in this paper the conformal mapping method is employed. Exact design equations, based on the conformal mapping solutions, for slit-coupled and broadside-coupled strip transmission lines are given in this section; these enable the designer to evaluate the physical line dimensions from the values of the characteristic impedances required by theoretical consideration. The details of the derivations of these equations will be described in the Appendix.

A. Design Equations for Slit-Coupled Strip Transmission Lines

In Table I orderly arrangements of the design equations for the two types of slit-coupled configuration shown in Fig. 4(a) and (b) are presented. By the use of these equations, cross sections are designed in a straightforward process to have the desired values of Z_{oe} and Z_{oo} when relative permittivity ϵ_r, ground-plane spacing b, and strip spacing s are given. Calculations may be carried out with the aid of the available tables [25]–[28] or rapidly converging ϑ functions [25]–[29].

In the design equations for the perpendicular slit-coupled configuration in Table I(b), it should be noted that the determinantal equation for the modulus k cannot be solved explicitly and, therefore, the graphical method is necessary only for the calculation of the value of k. Figure 6 is the plot of the relationship between the moduli k_o, giving the odd-mode characteristic impedance, and k, with s/b as a parameter. Using Fig. 6, the modulus k may be easily determined when the values of k_o and s/b are given. Furthermore, for the parallel slit-coupled configuration in Fig. 4(a), the results of computation using the design equations in Table I(a) are presented in nomogram form in Fig. 7(a)–(e) for the five selected values of s/b, the ratio of strip spacing to ground-plane spacing, in order to facilitate design.

TABLE I

DESIGN EQUATIONS FOR SLIT-COUPLED CONFIGURATIONS

	(a)	(b)
Cross Section	Parallel Case: Fig. 4(a)	Perpendicular Case: Fig. 4(b)
Dimensions	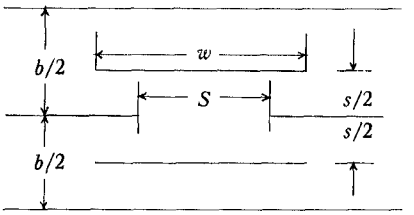	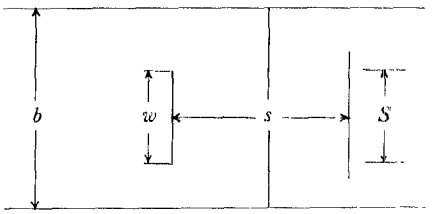
Values required by theoretical considerations	Z_{oe}, Z_{oo}	
Values to be selected	Relative permittivity ϵ_r, ground-plane spacing b, strip spacing s	
Characteristic Impedances	$\sqrt{\epsilon_r}\, Z_{oe} = 60\pi \dfrac{K'(k_e)}{K(k_e)}$, $\sqrt{\epsilon_r}\, Z_{oo} = 60\pi \dfrac{K'(k_o)}{K(k_o)}$	$\sqrt{\epsilon_r}\, Z_{oe} = 60\pi \dfrac{K(k_e)}{K'(k_e)}$, $\sqrt{\epsilon_r}\, Z_{oo} = 60\pi \dfrac{K(k_o)}{K'(k_o)}$
Modulus	$k = k_o$	$k_o = k\ \mathrm{cn}\ (s/b \cdot K')/\mathrm{dn}\ (s/b \cdot K')$
Parameters	$a = \dfrac{s}{b} K$	$a = \dfrac{s}{b} K'$
	$\beta = \mathrm{sn}^{-1}\ (k_e/k_o, k)$	$\beta = \mathrm{sn}^{-1}\left[\dfrac{1}{k'}\sqrt{1 - \left(\dfrac{k_o}{k_e}\right)^2}, k'\right]$
	$\alpha = \mathrm{sn}^{-1}\left[\dfrac{1}{k} \dfrac{\sqrt{Z(a)}}{\sqrt{Z(a)\ \mathrm{sn}^2 a + \mathrm{sn}\, a \cdot \mathrm{cn}\, a \cdot \mathrm{dn}\, a}}, k\right]$	$\alpha = \mathrm{sn}^{-1}\left[\dfrac{1}{k'}\sqrt{\mathrm{dn}^2 a - \dfrac{k^2 \cdot \mathrm{sn}\, a \cdot \mathrm{cn}\, a \cdot \mathrm{dn}\, a}{Z(a) + (\pi a/2KK')}}, k'\right]$
Dimensions	$\dfrac{w}{b} = \dfrac{1}{\pi} \log \dfrac{\Theta\ (\alpha + a)}{\Theta\ (\alpha - a)}$ $\dfrac{S}{b} = \dfrac{1}{\pi} \log \dfrac{H\ (\beta + a)}{H\ (\beta - a)}$	$\dfrac{w}{b} = \dfrac{1}{\pi}\left[\dfrac{\pi a}{KK'}\alpha - j \cdot \log \dfrac{\Theta_1\ (j\alpha + a)}{\Theta_1\ (j\alpha - a)}\right]$ $\dfrac{S}{b} = \dfrac{1}{\pi}\left[\dfrac{\pi a}{KK'}\beta - j \cdot \log \dfrac{\Theta\ (j\beta + a)}{\Theta\ (j\beta - a)}\right]$

Notes: Θ = Jacobian theta function.

H = Jacobian eta function.

Z = Jacobian zeta function.

sn, cn, and dn = Jacobian elliptic functions.

$K = \displaystyle\int_0^1 \frac{dt}{\sqrt{(1 - t^2)(1 - k^2 \cdot t^2)}}$ = complete elliptic integral of the first kind, with k as the modulus.

K' = complete elliptic integral of the first kind with complementary modulus $k'(=\sqrt{1-k^2})$.

$\mathrm{sn}^{-1}(\xi, k) = \displaystyle\int_0^\xi \frac{dt}{\sqrt{(1 - t^2)(1 - k^2 \cdot t^2)}} = F(\xi, k)$ = incomplete elliptic integral of the first kind.

$\Theta_1(u) = \Theta(K + u)$.

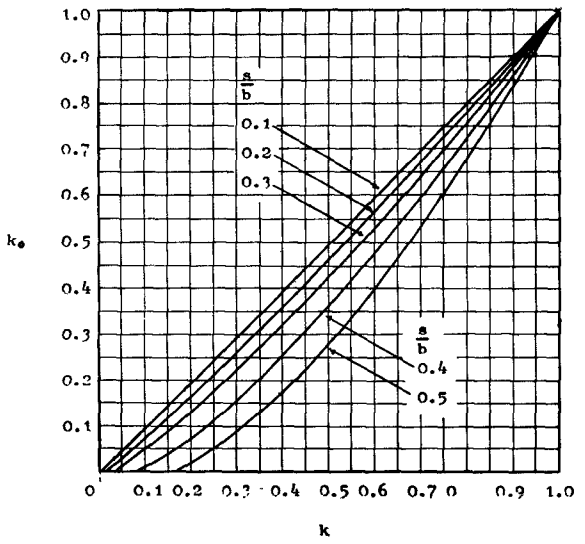

Fig. 6. Relationships between the moduli k_o and k in the determinantal equation for k in Table I(b).

Fig. 7. Nomograms giving the relative dimensions of the parallel slit-coupled configuration from the required values of Z_{oe} and Z_{oo}.

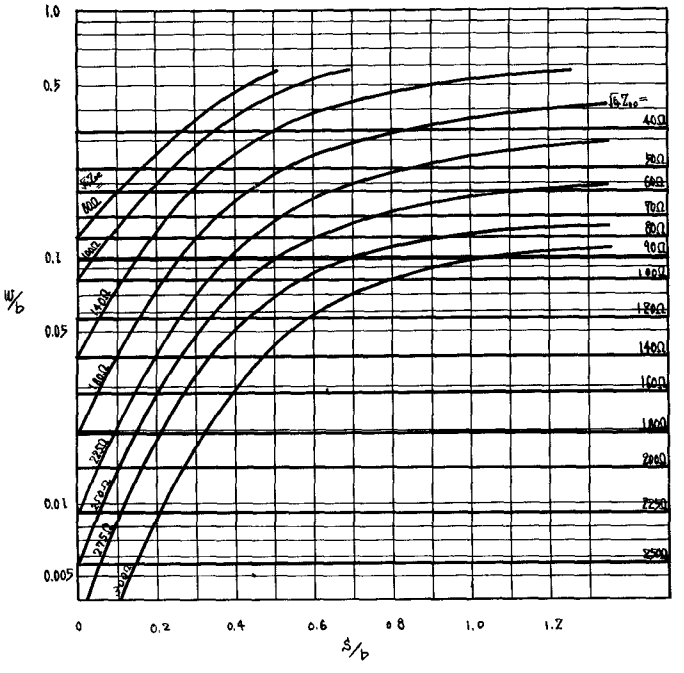

(a) $s/b=0.1$

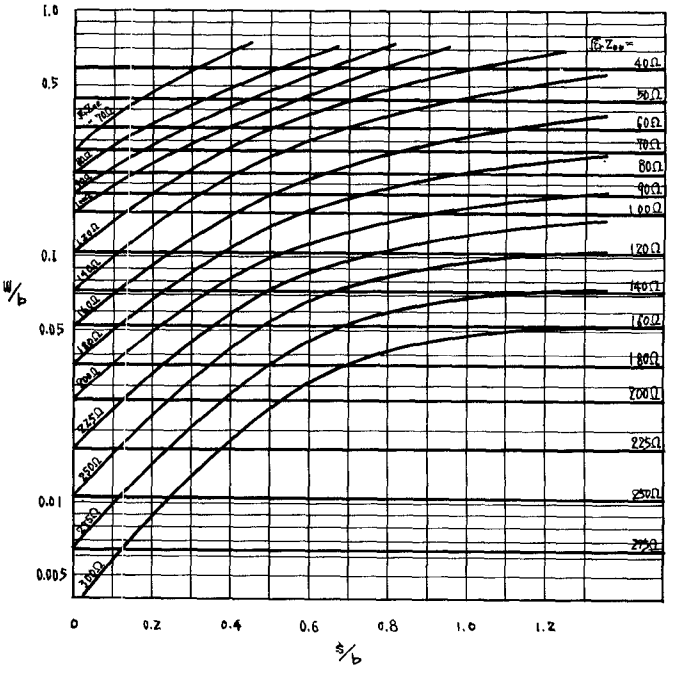

(b) $s/b=0.2$

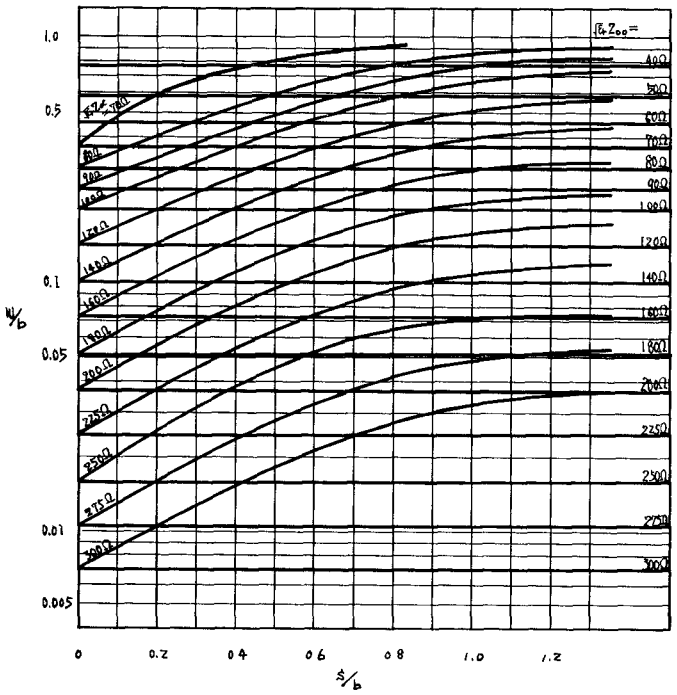

(c) $s/b = 0.3$

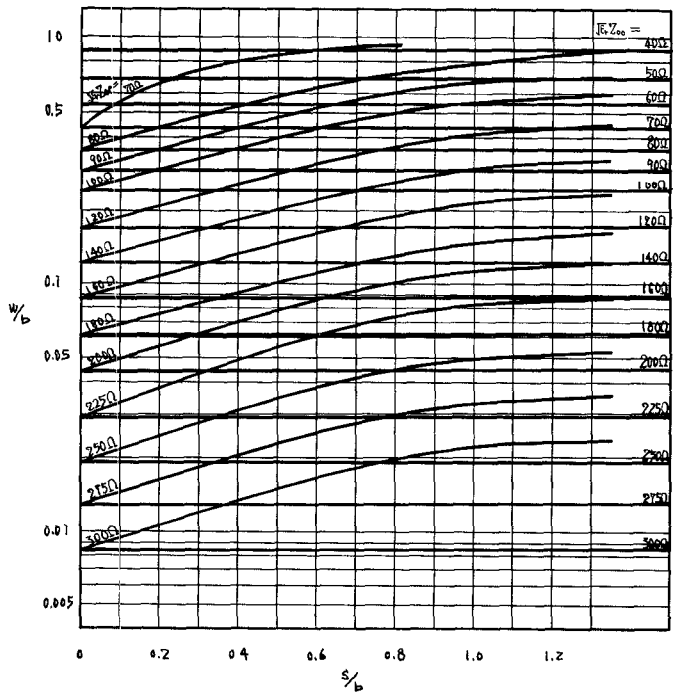

(d) $s/b = 0.4$

Fig. 7. (*Cont'd*)

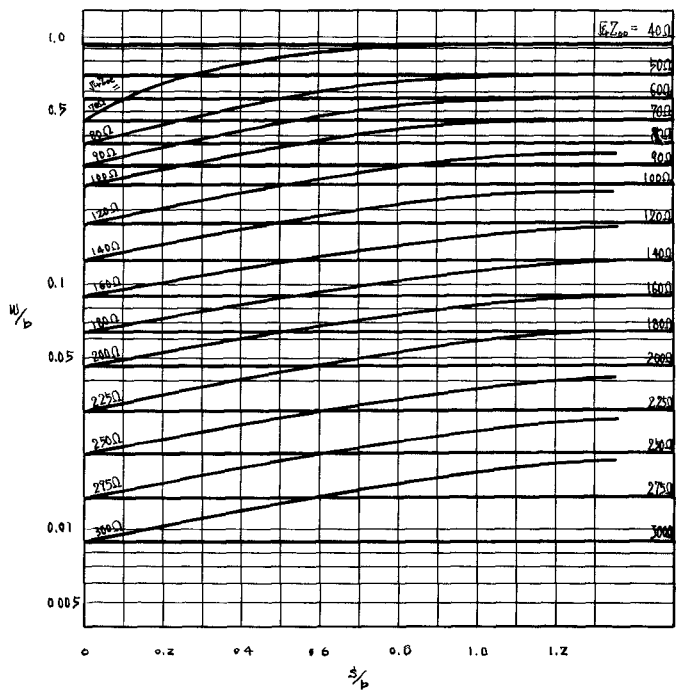

(e) $s/b = 0.5$

B. Design Equations for Broadside-Coupled Strip Transmission Lines

The broadside-coupled configurations in Fig. 2(a) and (b) are considered to be special cases of the slit-coupled configurations in Fig. 4(a) and (b), respectively. That is, the parallel configuration in Fig. 4(a) reduces to that in Fig. 2(a) for the limiting case $S \to \infty$; similarly, the perpendicular configuration in Fig. 4(b) reduces to that in Fig. 2(b) when S is equal to b. While broadside-coupled configurations are not suitable for the realization of the multisection components as previously described, one-section components often utilize these configurations because it is easy to achieve close coupling with less critical dimensions. Furthermore, the design equations for broadside-coupled configurations would be necessary in order to know the limitations on coupling of the slit-coupled configurations for the given values of strip spacing. Exact design equations for both parallel and perpendicular broadside-coupled strip configurations are presented in Table II. These equations result from modification of the equations in Table I. In both Table II(a) and (b), the graphical method is not necessary.

C. Design Equations for the Terminating Lines

In the design of many circuit components utilizing a parallel coupling effect, it is necessary to know the design equations for the terminating (or feeding) sections as well as for the coupled sections. The terminating lines to be connected to the coupled region may be constructed of single lines in isolation from each other. Design equations for the terminating lines are presented in Table III. The configuration in Table III(a) is to be used for the parallel case, while the other configurations in Table III are for the perpendicular case. The derivations of these equations are not given in this paper since they are easily obtained by the use of the design equations for the coupled configurations, as in Table I or Table II.

In the conventional components utilizing a parallel coupling effect, the bend or corner sections joining the terminating lines to the coupled region are employed in order to prevent undesirable coupling, and these bend or corner sections often cause an increase in the reflections. However, when the slit-coupled configurations are used, isolation between the terminating lines may be achieved without bends or corners by the use of the inner ground plate having no slit.

TABLE II

DESIGN EQUATIONS FOR BROADSIDE-COUPLED CONFIGURATIONS

	(a)	(b)
Cross Section	Parallel Case: Fig. 2(a)	Perpendicular Case: Fig. 2(b)
Dimensions	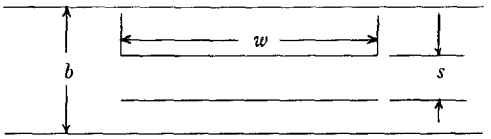	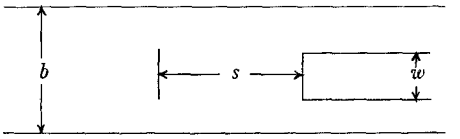
Characteristic Impedances	$\sqrt{\epsilon_r}\, Z_{oe} = 60\pi \dfrac{K'(k_e)}{K(k_e)}$, $\sqrt{\epsilon_r}\, Z_{oo} = 60\pi \dfrac{K'(k_o)}{K(k_o)}$	$\sqrt{\epsilon_r}\, Z_{oe} = 60\pi \dfrac{K(k_e)}{K'(k_e)}$, $\sqrt{\epsilon_r}\, Z_{oo} = 60\pi \dfrac{K(k_o)}{K'(k_o)}$
Modulus	$k = k_o$	$k = k_o/k_e$
Parameters	$a = \mathrm{sn}^{-1}(k_e/k_o, k)$	$a = \mathrm{sn}^{-1}(k_e'/k_o', k)$
	$\alpha = \mathrm{sn}^{-1}\left[\dfrac{1}{k} \dfrac{\sqrt{Z(a)}}{\sqrt{Z(a)\,\mathrm{sn}^2 a + \mathrm{sn}\, a \cdot \mathrm{cn}\, a \cdot \mathrm{dn}\, a}}, k\right]$	$\alpha = \mathrm{sn}^{-1}\left[\dfrac{1}{k'} \sqrt{\mathrm{dn}^2 a - \dfrac{k^2\, \mathrm{sn}\, a \cdot \mathrm{cn}\, a \cdot \mathrm{dn}\, a}{Z(a) + (\pi a/2KK')}}, k'\right]$
Dimensions	$\dfrac{w}{b} = \dfrac{1}{\pi} \log \dfrac{\Theta(\alpha + a)}{\Theta(\alpha - a)}$ $\dfrac{s}{b} = \dfrac{a}{K}$	$\dfrac{w}{b} = \dfrac{1}{\pi}\left[\dfrac{\pi a}{KK'} - j \log \dfrac{\Theta_1(j\alpha + a)}{\Theta_1(j\alpha - a)}\right]$ $\dfrac{s}{b} = \dfrac{a}{K'}$

Notes: $k_e' = \sqrt{1 - k_e^2}$

$k_o' = \sqrt{1 - k_o^2}$

TABLE III
DESIGN EQUATIONS FOR THE TERMINATING LINES

	(a)	(b)	(c)
Cross Section Dimensions	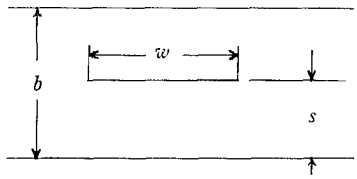	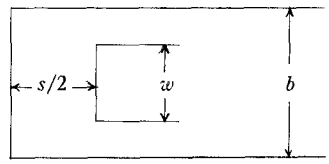	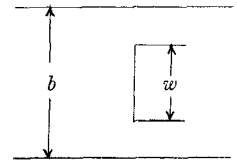
Characteristic Impedance	$\sqrt{\epsilon_r}\, Z_{os} = 60\pi \dfrac{K'(k_s)}{K(k_s)}$	$\sqrt{\epsilon_r}\, Z_{os} = 60\pi \dfrac{K(k_s)}{K'(k_s)}$	$\sqrt{\epsilon_r}\, Z_{os} = 30\pi \dfrac{K(k_s)}{K'(k_s)}$
Modulus	$k = k_s$	$k_s = k\dfrac{\mathrm{cn}(s/b \cdot K')}{\mathrm{dn}(s/b \cdot K')}$	
Parameters	$a = \dfrac{s}{b}K$ $\alpha = \mathrm{sn}^{-1}\left[\dfrac{1}{k}\dfrac{\sqrt{Z(a)}}{\sqrt{Z(a)\,\mathrm{sn}^2 a + \mathrm{sn}\,a \cdot \mathrm{cn}\,a \cdot \mathrm{dn}\,a}}\right]$	$a = \dfrac{s}{b}K'$ $\alpha = \mathrm{sn}^{-1}\left[\dfrac{1}{k'}\sqrt{\mathrm{dn}^2 a - \dfrac{k^2\,\mathrm{sn}\,a \cdot \mathrm{cn}\,a \cdot \mathrm{dn}\,a}{Z(a) + (\pi a/2KK')}},\ k'\right]$	
Strip Width	$\dfrac{w}{b} = \dfrac{2}{\pi}\log\dfrac{\Theta(\alpha + a)}{\Theta(\alpha - a)}$	$\dfrac{w}{b} = \dfrac{1}{\pi}\left[\dfrac{\pi a}{KK'}\alpha - j \cdot \log\dfrac{\Theta_1(j\alpha + a)}{\Theta_1(j\alpha - a)}\right]$	$\dfrac{w}{b} = \dfrac{2}{\pi}\cos^{-1} k_s$

CONCLUSIONS

Two types of slit-coupled configuration have been proposed and the exact design equations, based on the conformal mapping solutions, have been given in forms convenient for numerical calculation. The nomograms that enable us to determine the physical line dimensions from the desired values of the characteristic impedances for the parallel configuration have also been presented Furthermore, the exact design equations for the broadside-coupled configurations and the terminating lines have been given.

APPENDIX

A. Derivation of the Design Equations for Slit-Coupled Configurations

1) Parallel case, Fig. 4(a): It is convenient to bisect the complete cross section in Fig. 4(a) along the axis of symmetry parallel to the ground planes in order to simplify the analysis. Figure 8 shows the successive transformations used in the derivation of the design equations for the parallel slit-coupled configuration. Electric walls are indicated by the solid lines and magnetic walls by the dotted lines. The solid line between D and E and that between D′ and E′ are to be used for the odd-mode analysis, while the dotted lines are to be used for the even-mode analysis.

By means of the Schwarz-Christoffel method, the integral equation relating the z- and t-planes in Fig. 8 is found to be

$$z = C_1 \int_0^t \frac{(t^2 - \mathrm{sn}^2\,\alpha)\,dt}{\sqrt{(1 - t^2)(1 - k^2t^2)\,(1 - t^2k^2\,\mathrm{sn}^2\,a)}} + C_2 \quad (3)$$

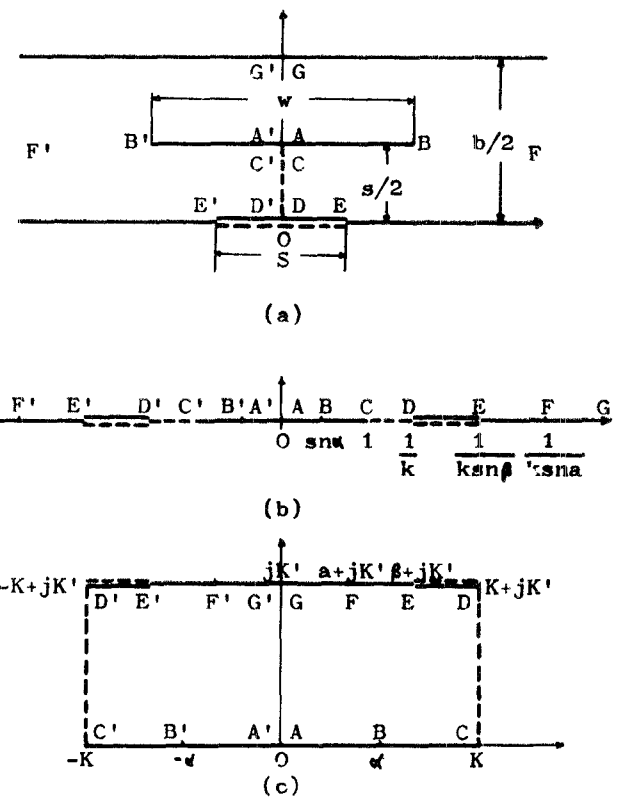

Fig. 8. Transformations for the parallel slit-coupled configuration in Fig. 4(a). (a) z-plane. (b) t-plane. (c) u-plane.

where C_1 and C_2 are constants to be determined. In order to evaluate this integral, the upper half of the t-plane in Fig. 8(b) is mapped onto the interior of a rectangle on the u-plane in Fig. 8(c) by

$$t = \mathrm{sn}\ (u, k). \tag{4}$$

Then the mapping function from the z- to the u-plane can be obtained by substituting (4) in (3) and applying the boundary conditions, as

$$z = \frac{b}{2\pi} \cdot \log \frac{\Theta\ (u + a)}{\Theta\ (u - a)} + j \cdot \frac{s}{2} \tag{5}$$

under the following condition:

$$\mathrm{sn}^2\ \alpha = \frac{1 - k^2\ \mathrm{sn}^2\ a \cdot \mathrm{sn}^2\ \alpha}{k^2 \cdot \mathrm{sn}\ a \cdot \mathrm{cn}\ a \cdot \mathrm{dn}\ a} Z(a). \tag{6}$$

Equation (6) results from the condition that A and C (or A' and C') must coincide in the z-plane in Fig. 8(a). In the above equations the terms sn, cn, dn are the Jacobian elliptic functions, k is the modulus, and the terms Θ and Z are the Jacobian theta and zeta functions [29], respectively. Solving (6) for α gives the determinantal equation for α in Table I(a). Next, the cross-section dimensions in the z-plane must be related to the corresponding values in the u-plane by the use of (5).

Applying some boundary conditions gives

$$\frac{s}{b} = \frac{a}{K}, \tag{7}$$

$$\frac{w}{b} = \frac{1}{\pi} \log \frac{\Theta\ (\alpha + a)}{\Theta\ (\alpha - a)}, \tag{8}$$

$$\frac{S}{b} = \frac{1}{\pi} \log \frac{H(\beta + a)}{H(\beta - a)}. \tag{9}$$

In (7)–(9), K is the complete elliptic integral of the first kind, with k as the modulus, and the term H is the Jacobian eta function [29] defined by

$$H(u) = -j \cdot q^{1/4} \exp\left(j \frac{u}{2K} \pi\right) \Theta(u + jK') \tag{10}$$

where

$$q = \exp\left(-\pi \frac{K'}{K}\right), \tag{11}$$

and where K' is the complete elliptic integral of the first kind with the complementary modulus $k'(=\sqrt{1-k^2})$. Now consider the odd-mode. It can be seen that the u-plane structure in Fig. 8(c) is the parallel-plate condenser with no fringing effect. Then the odd-mode static capacitance of one strip to ground is easily obtained by adding subscript o to the modulus to denote the odd-mode, as

$$\frac{C_{oo}}{\epsilon} = \frac{2K(k_o)}{K'(k_o)}, \tag{12}$$

where

$$k_o = k. \tag{13}$$

In the even-mode, the upper-half of the t-plane in Fig. 8(b) is mapped onto the interior of the ideal parallel-plate condenser, as in the odd-mode, by

$$t = \mathrm{sn}\ (u, k_e) \tag{14}$$

where

$$k_e = k \cdot \mathrm{sn}\ \beta. \tag{15}$$

Then the even-mode capacitance of one strip to ground is

$$\frac{C_{oe}}{\epsilon} = \frac{2K(k_e)}{K'(k_e)} \tag{16}$$

where subscript e is added to k to denote the even-mode.

Substitution of (12) and (16) in (1) yields the odd- and even-mode characteristic impedance, respectively. In Table I(a), the equations derived above are listed after suitable modification.

2) Perpendicular case, Fig. 4(b): The mapping procedure for the perpendicular slit-coupled configuration in Fig. 4(b) is similar to that used for the parallel case. By virtue of the two planes of symmetry, we need consider in detail only one quadrant of the complete cross section in Fig. 4(b). The successive transformations used for this case are shown in Fig. 9, where the following simplified notations are used:

$$\begin{aligned} \mathrm{sn}\ \beta' &= \mathrm{sn}\ (\beta, k') \\ \mathrm{cn}\ \beta' &= \mathrm{cn}\ (\beta, k') \\ \mathrm{dn}\ \alpha' &= \mathrm{dn}\ (\alpha, k') \end{aligned} \tag{17}$$

where

$$k' = \sqrt{1 - k^2}.$$

In this case, the mapping function relating the z- and u-planes is found to be, using the Schwarz-Christoffel method,

$$z = \frac{b}{2\pi} \left\{ \log \frac{\Theta\ (u + a)}{\Theta\ (u - a)} + \frac{\pi a}{KK'} u \right\}, \tag{18}$$

under the following condition:

$$K' = \frac{\mathrm{dn}^2\ \alpha' - k^2\ \mathrm{sn}^2\ a}{k^2\ \mathrm{sn}\ a \cdot \mathrm{cn}\ a \cdot \mathrm{dn}\ a} \left\{ K' Z(a) + \frac{\pi a}{2K} \right\}, \tag{19}$$

by the use of the transformation from the t- to the u-plane by the function

$$t = \mathrm{sn}\ (u, k), \tag{4}$$

as in the parallel case.

The determinantal equation for α in Table I(b)results from (19). Substitution of the corresponding values in the z- and u-planes in Fig. 9 in (18) leads to the following results:

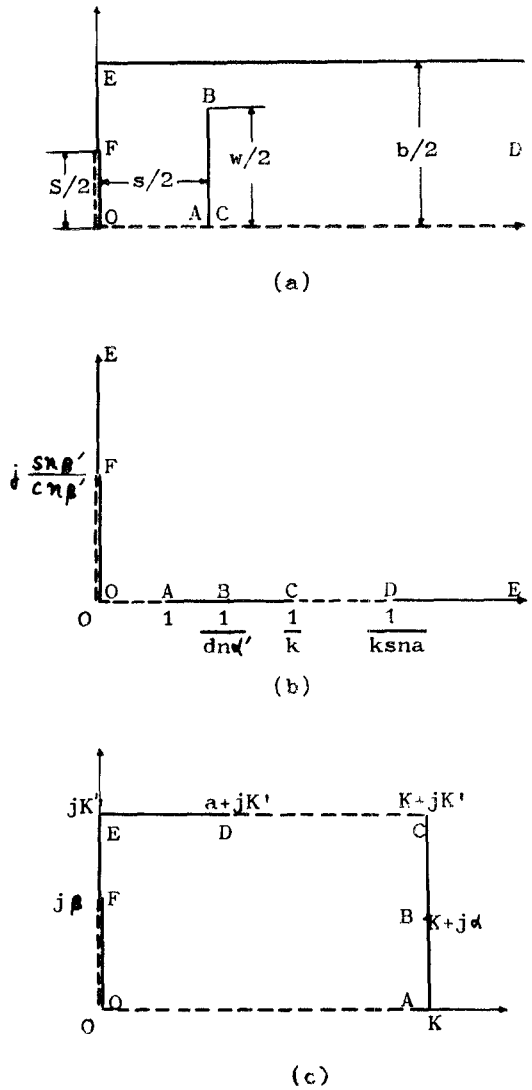

Fig. 9. Transformations for the perpendicular slit-coupled configuration in Fig. 4(b). (a) z-plane. (b) t-plane. (c) u-plane.

$$\frac{s}{b} = \frac{a}{K'}, \tag{20}$$

$$\frac{w}{b} = \frac{1}{\pi}\left\{\frac{\pi a}{KK'}\alpha - j\log\frac{\Theta(K + j\alpha + a)}{\Theta(K + j\alpha - a)}\right\}, \tag{21}$$

$$\frac{S}{b} = \frac{1}{\pi}\left\{\frac{\pi a}{KK'}\beta - j\log\frac{\Theta(j\beta + a)}{\Theta(j\beta - a)}\right\}, \tag{22}$$

where the second terms of the right-hand sides of (21) and (22) are real [25]. Thus, the physical dimensions of the structure in Fig. 4(b) have been related to the u-plane parameters by (20)–(22).

Now, it is necessary to transform the t-plane in Fig. 9(b) to the ideal parallel-plate representation for both the odd- and the even-mode. For the odd-mode, the solid line (electric wall) between F and O on the planes of Fig. 9 must be used. The first quadrant of the t-plane in Fig. 9(b) is mapped into the first quadrant of the t'-plane, and finally to the interior of a rectangle on the v-plane as shown in Fig. 10. The mapping functions are

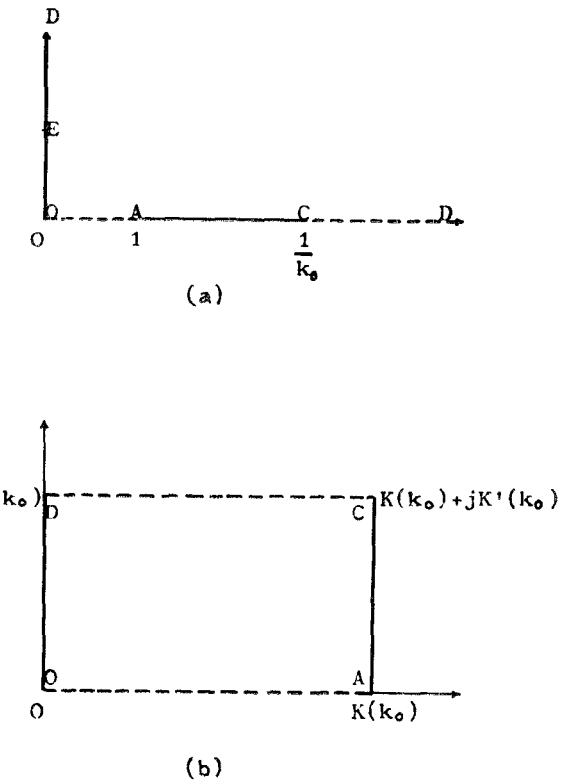

Fig. 10. Transformations from t-plane in Fig. 9(b) for odd-mode. (a) t'-plane. (b) v-plane.

$$t'^2 = \frac{t^2 \cdot \mathrm{dn}^2\, a}{1 - t^2 \cdot k^2\, \mathrm{sn}^2\, a} \tag{23}$$

which moves D to infinity in the t'-plane, and

$$t' = \mathrm{sn}\,(v, k_o). \tag{24}$$

Referring to the v-plane structure, the odd-mode capacitance of one strip to ground is

$$\frac{C_{oo}}{\epsilon} = \frac{2K'(k_o)}{K(k_o)}. \tag{25}$$

Now the corresponding values in the t- and t'-planes are substituted in (23) to give

$$k_o = k\,\frac{\mathrm{cn}\, a}{\mathrm{dn}\, a}. \tag{26}$$

From (20) and (26) we get the determinantal equation for the modulus k in Table I(b).

Next we consider the even-mode. Transformations from the t-plane in Fig. 9(b) are shown in Fig. 11.

The mapping functions are

$$t'^2 = \frac{\mathrm{dn}^2\, a(\mathrm{sn}^2\, \beta' + t^2\, \mathrm{cn}^2\, \beta')}{1 - t^2 k^2\, \mathrm{sn}^2\, a} \tag{27}$$

which moves F to the origin and D to infinity in the t'-plane in Fig. 11(a), and

$$t' = \mathrm{sn}\,(v, k_e). \tag{28}$$

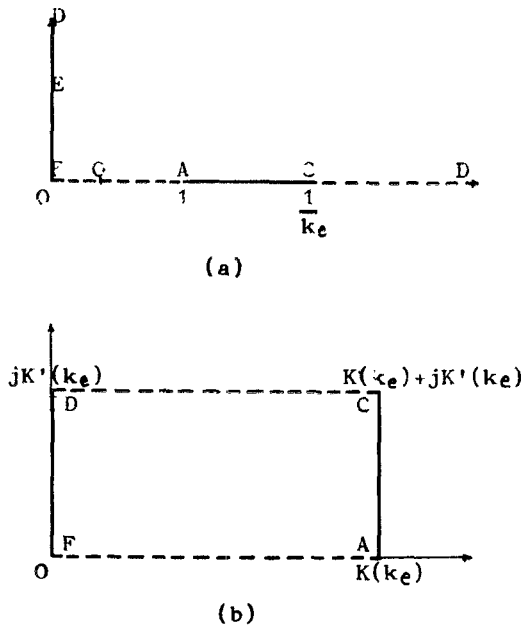

Fig. 11. Transformations from t-plane in Fig. 9(b) for even-mode. (a) t'-plane. (b) v-plane.

Then the even-mode capacitance of one strip to ground is

$$\frac{C_{oe}}{\epsilon} = \frac{2K'(k_e)}{K(k_e)} \tag{29}$$

and the modulus k_e is

$$k_e = k \frac{\text{cn } a}{\text{dn } a} \frac{1}{\text{dn } \beta'} \tag{30}$$

where

$$\text{dn } \beta' = \text{dn } (\beta, k'). \tag{31}$$

From (26) and (30), we get

$$\text{dn } \beta' = \frac{k_o}{k_e}. \tag{32}$$

Modification of (32) yields the determinantal equation for β in Table I(b). Thus the necessary equations have been derived. These are listed in Table I(b) after an orderly arrangement.

B. Comments on the Derivations of the Design Equations for the Broadside-Coupled Configurations

Design equations for the parallel broadside-coupled configuration in Fig. 2(a) are derived by letting $\beta = a$ in those for the parallel slit-coupled configuration. Then, from (13) and (15), the determinantal equation for a is found to be

$$\text{sn } (a, k) = \frac{k_e}{k_o}. \tag{33}$$

All other equations are exactly the same for the parallel broadside-coupled case as for the parallel slit-coupled case in Table I(a).

For the perpendicular broadside-coupled configuration, design equations are derived by letting $\beta = K'$ in those for the perpendicular slit-coupled configuration.

Since $\text{dn}(K', k') = k$, we get from (31) and (32)

$$k = \frac{k_o}{k_e} \tag{34}$$

which is the determinantal equation for the modulus k. Furthermore, the determinantal equation for a is

$$\text{sn } (a, k) = \sqrt{\frac{1 - k_e^2}{1 - k_o^2}}. \tag{35}$$

This results from (26) and (34).

All other equations are exactly the same for this case as for the perpendicular slit-coupled case in Table I(b).

Acknowledgment

The authors wish to thank K. Sawai who programmed and ran the computer.

References

[1] E. M. T. Jones and J. T. Bolljahn, "Coupled-strip-transmission-line filters and directional couplers," *IRE Trans. on Microwave Theory and Techniques*, vol. MTT-4, pp. 75–81, April 1956.
[2] S. B. Cohn, "Parallel-coupled transmission-line-resonator filters," *IRE Trans. on Microwave Theory and Techniques*, vol. MTT-6, pp. 223–231, April 1958.
[3] H. Ozaki and J. Ishii, "Synthesis of a class of strip-line filters," *IRE Trans. on Circuit Theory*, vol. CT-5, pp. 104–109, June 1958.
[4] N. Saito, "A coupled transmission-line filter (The design method by means of extracting coupled lines from the prescribed circuit)" (in Japanese), *J. Inst. Elec. Commun. Engrs. (Japan)*, vol. 44, pp. 1036–1040, July 1961.
[5] J. K. Shimizu and E. M. T. Jones, "Coupled transmission-line directional couplers," *IRE Trans. on Microwave Theory and Techniques*, vol. MTT-6, pp. 403–410, October 1958.
[6] K. Araki, "The characteristic impedance of the pair cable type directional coupler" (in Japanese), *J. Inst. Elec. Commun. Engrs. (Japan)*, vol. 45, pp. 58–64, January 1962.
[7] R. Levy, "General synthesis of asymmetric multi-element coupled-transmission-line directional couplers," *IEEE Trans. on Microwave Theory and Techniques*, vol. MTT-11, pp. 226–237, July 1963.
[8] P. P. Toulios and A. C. Todd, "Synthesis of symmetrical TEM-mode directional couplers," *IEEE Trans. on Microwave Theory and Techniques*, vol. MTT-13, pp. 536–544, September 1965.
[9] E. G. Cristal and L. Young, "Theory and tables of optimum symmetrical TEM-mode coupled-transmission-line directional couplers," *IEEE Trans. on Microwave Theory and Techniques*, vol. MTT-13, pp. 544–558, September 1965.
[10] F. S. Coale, "A traveling-wave directional filter," *IRE Trans. on Microwave Theory and Techniques*, vol. MTT-4, pp. 256–260, October 1956.
[11] K. Kuroda, "Design consideration for a traveling-wave directional filter" (in Japanese), presented at the 1958 Professional Conf. on Circuit Theory of the Inst. of Elec. Commun. Engrs. (Japan).
[12] J. Ishii, "On the design of strip-line channel separation filters" (in Japanese), presented at the 1958 Joint Meeting of the Four Electrical Institutes of Japan, no. 1.
[13] B. M. Schiffman, "A new class of broad-band microwave 90-degree phase shifters," *IRE Trans. on Microwave Theory and Techniques*, vol. MTT-6, pp. 232–237, April 1958.
[14] W. J. D. Steenaart, "The synthesis of coupled transmission line all-pass networks in cascades of 1 to n," *IEEE Trans. on Microwave Theory and Techniques*, vol. MTT-11, pp. 23–29, January 1963.
[15] J. Ishii, "The design of UHF delay equalizing network" (in Japanese), presented at the 1960 Joint Meeting of the Four Electrical Institutes of Japan, no. 52.

[16] E. M. T. Jones, "Wide-band strip-line magic-T," *IRE Trans. on Microwave Theory and Techniques*, vol. MTT-8, pp. 160–168, March 1960.
[17] D. I. Kraker, "Asymmetric coupled-transmission-line magic-T," *IEEE Trans. on Microwave Theory and Techniques*, vol. MTT-12, pp. 595–599, November 1964.
[18] K. Itakura, S. Yamamoto, and T. Azakami, "Coupled strip-line hybrid circuit" (in Japanese), presented at the 1966 Joint Meeting of the Four Electrical Institutes of Japan, no. 1069.
[19] S. B. Cohn, "Characteristic impedances of broadside-coupled strip transmission lines," *IRE Trans. on Microwave Theory and Techniques*, vol. MTT-8, pp. 633–637, November 1960.
[20] T. Ikeda and R. Sato, "Characteristic impedances of broadside-coupled strips parallel to the ground planes" (in Japanese), presented at the 1965 Joint Meeting of the Four Electrical Institutes of Japan, no. 1459.
[21] W. J. Getsinger, "A coupled strip-line configuration using printed-circuit construction that allows very close coupling," *IRE Trans. on Microwave Theory and Techniques*, vol. MTT-9, pp. 535–544, November 1961.
[22] J. P. Shelton, "Impedances of offset parallel-coupled strip transmission lines," *IEEE Trans. on Microwave Theory and Techniques*, vol. MTT-14, pp. 7–15, January 1966.
[23] T. Arakawa, "Edge effect correcting method" (in Japanese), *Reports of University of Electro-Communications, Tokyo*, no. 5, December 1953.
[24] S. B. Cohn, "Thickness corrections for capacitive obstacles and strip conductors," *IRE Trans. on Microwave Theory and Techniques*, vol. MTT-8, pp. 638–644, November 1960.
[25] G. W. Spenceley and R. M. Spenceley, *Smithsonian Elliptic Functions Tables*, Smithsonian Miscellaneous Collections, vol. 109, Washington, D.C.: Smithsonian Institute, 1947.
[26] F. Oberhettinger and W. Magnus, *Anwendung der Elliptischen Funktionen in Physik und Technik*. Berlin: Springer-Verlag, 1949.
[27] L. M. Milne-Thomson, *Die Elliptischen Funktionen von Jacobi*. New York: Dover, 1950, Tables (reprint).
[28] H. Nagaoka and S. Sakurai, "Tables of theta functions, elliptic integrals K and E, and associated coefficients in the numerical calculation of elliptic functions," Table 1, vol. II, *Scientific Papers of the Institute of Physical and Chemical Research*, Tokyo, Japan, 1922.
[29] S. Tomochika, *Elliptic Functions* (in Japanese). Tokyo: Kyoritsu, 1958.

Some Designs of X_L-Band Diode Switches

R. N. ASSALY

Abstract—X_L-band waveguide switches, using PIN diodes for the switching elements, were developed in the SPST, SP2T, SP4T, and SP8T configurations. At the frequency of 7.75 GHz, for which they were tuned, they exhibited insertion losses on the average of 0.1, 0.4, 0.6, and 1.1 dB, respectively. In all cases, the signal going out of each switch port when turned OFF decreased in excess of 29 dB. The bandwidth of each switch, whose values are indicated, is narrower for the switch which has the larger number of ports or which contains diodes of lower capacitance. Semiempirical formulas are developed which predict performance characteristics of the SPST switch in particular.

I. Introduction

MICROWAVE SWITCHES, which are operated by the action of diodes, are used increasingly in microwave systems because of their valuable advantages of light weight and low driving (or bias) power. In the X-band region, only SPST switches are reported in the literature [1]–[10] (to this writer's knowledge) and a few SP2T and (special-order) SP4T switches are available commercially [11]. The limitations encountered in the design of the multithrow switch are primarily due to RF losses. The switch, in essence, consists of a number of SPST units mounted in a transmission line junction, and its loss is the combined loss of all the SPST units as well as the junction. Those SPST switches that were reported had insertion losses in the ON state in excess of 1/2 dB and generally about 1 dB. In the OFF state, insertion losses ranged as low as 20 dB (which also represents a loss in the multithrow switch). Some high insertion losses have been achieved but at the expense of bandwidth or high insertion loss in the ON state. To design a multithrow switch with good characteristics is contingent upon the development of an SPST unit with correspondingly better characteristics in both the ON and OFF states.

The switches in this paper were developed for a specific application where they had to give their best performance at 7.75 GHz in the X_L-band region and had to have a broad bandwidth. However, this should not limit their usefulness, for the principles set forth are applicable in general.

The SPST switch will be described first, followed by the SP4T, the SP2T, and the SP8T switch. Before the switches could be developed in detail, however, it was necessary to make educated guesses as to which basic designs would produce the best characteristics, as will be outlined in the following section. The descriptions in this paper are for the small-signal application. Measurements to determine the dependence of a switch characteristic on the RF power level or the power limitations will not be reported.

Manuscript received March 1, 1966; revised August 2, 1966.
The author is with the M. I. T. Lincoln Laboratory, Lexington, Mass. (Operated with support from the U. S. Air Force.)